



Published in final edited form as:

J Clin Psychiatry. ; 79(6): . doi:10.4088/JCP.18m12106.

Trajectories in Cerebral Blood Flow Following Antidepressant Treatment in Late-life Depression: Support for the Vascular Depression Hypothesis

Wenjing Wei, MD^{1,2}, Helmet T. Karim, PhD³, Chemin Lin, MD^{4,5}, Akiko Mizuno, PhD³, Carmen Andreescu, MD³, Jordan F. Karp, MD³, Charles F. Reynolds III, MD³, and Howard J. Aizenstein, MD, PhD^{3,6}

¹The Third Xiangya Hospital of Central South University, Changsha, Hunan, China

²University of Pittsburgh School of Medicine, Pittsburgh, Pennsylvania, United States of America

³Department of Psychiatry, University of Pittsburgh, Pittsburgh, Pennsylvania, United States of America

⁴Department of Psychiatry, Keelung Chang Gung Memorial Hospital, Keelung, Taiwan

⁵College of Medicine, Chang Gung University, Taoyuan, Taiwan

⁶Department of Bioengineering, University of Pittsburgh, Pittsburgh, Pennsylvania, United States of America

Abstract

Objective: Studies have identified longitudinally that there exists an association between depression, cerebral blood flow (CBF), and white matter hyperintensities (WMH) that are thought to be due to vascular pathologies in the brain. However, the changes in CBF, a measure that reflects cerebrovascular integrity, following pharmacotherapy are not well understood. In this study, we investigated the dynamic CBF changes over the course of antidepressant treatment, and its association with depressive symptoms.

Methods: We used pseudo-continuous arterial spin labeling (pCASL) to investigate CBF changes in a sample of older depressed patients (N=46, 29 female) with DSM-IV diagnosis of major depressive disorder (MDD). Participants had five magnetic resonance imaging (MRI) scans [baseline, following a placebo, following a single dose of venlafaxine, a week after starting venlafaxine, and at the end of trial (12 weeks)]. Montgomery-Åsberg Depression Rating Scale (MADRS) was used to evaluate depression severity and treatment outcome. We investigated the association between changes in depression severity with changes in voxel-wise CBF while adjusting for potential confounding factors.

Results: Increased CBF in the middle and posterior cingulate between baseline and end of treatment was significantly associated with percent decrease of MADRS, independent of sex and

Corresponding Author: Howard J. Aizenstein, MD, PhD, Western Psychiatric Institute and Clinic, 3811 O'Hara Street, Pittsburgh, PA 15213, Tel: (412) 246-5464, aizen@pitt.edu.

NCT00892047 and NCT01124188

mini-mental status exam (MMSE) score (5000 permutations, cluster forming threshold $p < 0.005$, family-wise error $p < 0.05$). No significant effects were detected between baseline and other scans (i.e., placebo, acute (single dose), or sub-acute (after a week)).

Conclusion: Regional CBF increases significantly post-treatment and was associated with decreases in depressive symptoms. This observation is consistent with the vascular depression hypothesis in late-life depression.

Keywords

LLD; CBF; Vascular Depression Hypothesis; Treatment

Introduction

Depression is a leading cause of global burden of illness-related disability^{1,2}, affecting up to 16% of older adults³⁻⁵. Treatment response of depression is approximately 50 percent⁶⁻⁸ and treatment resistance is common, such that patients frequently need multiple trials before finding an effective treatment⁹. This delay increases the risk for suicide, medical comorbidity, disability, and family caregiving burden especially in older adults¹⁰.

Thus, identifying biomarkers of treatment response variability is important to improving treatment outcomes in late-life depression (LLD). While several putative structural and functional neuroimaging markers of treatment response have been reported¹¹⁻¹⁶, most of these are static markers identified at the initiation of treatment. We currently have limited knowledge about dynamic markers of response, or how physiological changes early in treatment predict final response. Recently, our group has shown that changes in resting blood-oxygen-level dependent (BOLD) connectivity differ depending on treatment response and can occur as early as one day after exposure to antidepressant medication¹⁷. However, the BOLD signal may not be the only dynamic marker associated with treatment response.

The vascular depression hypothesis states that cerebrovascular disease may predispose, precipitate, or perpetuate some geriatric depressive syndromes¹⁸. The major conceptual driver may be small vessel disease leading to white matter hyperintensities (WMH)¹⁹ in midline structures, ventricles, and cingulum that disrupt white matter connectivity²⁰ but also decreased CBF²¹. Together, this may support both a frontolimbic dysconnectivity hypothesis²² as well as driving functional differences due to decreased CBF²³, though it is possible that the reverse pattern is also true. In fact, this pattern (greater small vessel disease – worsened CBF – worsened neural functioning – greater depressive symptoms) may be highly circular and interdependent.

Given the association of vascular integrity and depression in older adults, measuring neurovascular function may provide clinically relevant insight on late-life depression. Arterial Spin Labeling (ASL) has been shown to be useful as a biomarker of brain response to antidepressants²⁴. Compared to the BOLD signal, ASL has the advantage that it is not confounded by blood volume or oxygen consumption²⁵.

Regional CBF alterations have been linked to major depressive disorder (MDD). Several studies have reported that, compared with non-depressed controls, mid-life and young adults with MDD have mixed CBF changes in multiple regions^{26–30}. However, these abnormalities may not characterize CBF in the elderly, given the anatomical and pathophysiological changes observed in the aging brain. Studies in LLD using positron emission tomography (PET) or single photon emission computed tomography (SPECT) have found that LLD individuals had lower regional CBF compared with non-depressed controls^{31–34}. The changes in CBF are especially salient in LLD within the theoretical framework of the vascular depression hypothesis that cerebrovascular disease may predispose, precipitate or perpetuate some geriatric depressive syndromes^{18,35,36}. Strictly speaking, the PET/SPECT mainly measures brain metabolism through tracer coupling, which reflects CBF in some degree and good agreement exists between PET/SPECT measurement and ASL measurement³⁷, but the invasiveness of PET/SPECT does not allow for repeated measurement in a relatively short time. The transcranial Doppler (TCD) mainly measures the velocity of the CBF in major vessels, which reflects the brain tissue pulsatility and vessel elasticity, but the actual CBF also depends on the diameter of the vessel and the TCD fails to provide voxel-wise information of deeper brain tissue. With the use of inner tracer and the subtraction of tagged and untagged images, the ASL measures CBF more directly and voxel-wise without introducing exposure to radiation. Finally, WMH may be a consequence of low CBF – however the reverse may also be true. There is very little research that focuses on this aspect of the causality of WMH and low CBF – however it is possible that since WMH are in part due to ischemia. Therefore, we investigated the changes associated with regional cerebral blood flow (CBF) alterations as measured by ASL.

For this study, we used pseudo-continuous ASL (pCASL) to investigate dynamic gray matter CBF changes in older depressed patients receiving antidepressant pharmacotherapy. We measured whole brain CBF at baseline, after placebo, and then at three different time points (a single dose, a week after, and at the end of trial) during a 12-week open-label venlafaxine treatment trial. As per the vascular depression model, we predicted that depression remission would be associated with increased CBF in gray matter. As LLD has been associated with multiple gray matter regions across the brain, we used a voxel-wise approach to characterize where in the gray matter the ASL changes occurred.

Methods

Participants:

The present study recruited participants from the open-label phase of two longitudinal clinical trials (IRL-GREY³⁸ and ADAPT³⁹: NCT00892047 and NCT01124188, respectively) and all data were collected between July 2011 and December 2015. All participants (at least 50 years old) met DSM-IV (Diagnostic and Statistical Manual of Mental Disorders IV) criteria for major depressive disorder (MDD) and had Montgomery-Åsberg Depression Rating Scale (MADRS) scores of at least 15 at the time of scanning. Exclusion criteria were any history of mania or psychosis, alcohol or substance abuse (last three months), or disease with known effects on mood (e.g. dementia, stroke, multiple sclerosis, vasculitis, significant head trauma, unstable hypertension, or diabetes), current

psychotic symptoms, uncontrolled medical illnesses, contraindication to venlafaxine XR, or ineligibility for magnetic resonance imaging (MRI) (e.g. implanted metal, overweight, claustrophobia, or pregnancy). Participants were involved in a 12-week treatment trial for venlafaxine, and MRI was performed at five time points: baseline, a day after receiving a placebo, a day after receiving the first dose of venlafaxine, a week following continued medication, and at the end of the trial (Figure 1). Patients started initially on 37.5mg/day, increased by 37.5mg up to 150mg/day, those that did not respond at week 6 had their target increased to 300mg/day (Detailed dosage information³⁸).

Older participants (N=58) provided written informed consent with both the current protocol as well as the clinical trials they were enrolled in, which were all approved by the University of Pittsburgh institutional review board. Twelve participants were excluded due to drug side effects (N=5), in-scanner anxiety (N=1), no MRI (N=2), missing behavioral data (N=1), loss of communication (N=2), and no desire to complete the end of trial scan (N=1). Thus, 46 participants were included in the final analysis and had all neuroimaging and behavioral data at each time point.

Clinical Assessments:

After collecting demographic and clinical information, the Cumulative Illness Rating Scale for Geriatrics (CIRSG)⁴⁰ and Mini-Mental Status Examination (MMSE)⁴¹ were administered. Remission was defined as MADRS less than 10 for at least two consecutive weeks that lasted through the trial.

Clinicians saw participants once a week for the first two weeks and then every two weeks. On scanning dates blood samples were taken to measure venlafaxine serum levels.

Image acquisition:

All scanning was conducted in the morning at the MR research center with a 3 Tesla Siemens Trio scanner (Munich, Germany) and a 12-channel head coil.

The scanner removed initial dummy scans. Structural data was collected at baseline and end scans. An axial, whole brain T1-weighted magnetization-prepared rapid gradient echo (MPRAGE) sequence was collected with echo time (TE)=3.43ms, repetition time (TR)=2300ms, flip angle (FA)=9 degrees, inversion time (TI)=900ms, field of view (FOV)=256×224, 176 slices, and 1mm isotropic resolution. An axial, whole brain T2-weighted fluid attenuated inversion recovery (FLAIR) sequence was also collected with TE=90ms, TR=9160 ms, FA=150 degrees, TI=2500ms, FOV=256×212, 48 slices, and 1×1×3mm resolution.

An axial, whole brain (except cerebellum) resting state pseudo-continuous arterial spin labeling (pCASL) sequence was collected. Participants were instructed to keep eyes open and fixated on a cross hair and to stay awake. The sequence lasted for approximately five minutes and with TE=13ms, TR=4000ms, FA=90 degrees, FOV=64×64, 32 slices, 80 total tagged and untagged volumes, and 4mm isotropic resolution.

Preprocessing and CBF calculation:

All preprocessing was performed with SPM12 (<http://www.fil.ion.ucl.ac.uk/spm/software/spm12/>) in MATLAB 2015b (MathWorks, Massachusetts, US) except where specifically mentioned. The interpolation used was a 4th degree B-spline interpolation and the similarity metrics were mutual information for images of the same type (e.g., between functional sequences) and normalized mutual information for images of differing types (e.g., between functional-structural).

For structural preprocessing, we coregistered the FLAIR to the MPRAGE, and then performed a multi-spectral segmentation into gray matter, white matter, cerebral spinal fluid (CSF), soft tissue, skull, and air (after light bias regularization). This segmentation outputs a deformation field that normalizes images into a standard anatomic space (Montreal Neurological Institute, MNI space). We generated an intracranial volume (ICV) mask by combining all voxels with probability greater than 0.1 in gray matter, white matter, or CSF then filling holes with the image filling algorithm (imfill), followed by an image closing algorithm to smooth out and close holes at the border (imclose). We skull stripped the MPRAGE and FLAIR using the mask. Structural volumes were normalized and then calculated the mean across participants to overlay neuroimaging results.

White matter hyperintensities (WMHs) were segmented using FLAIR images with a previously established automatic algorithm⁴². WMH probability map was generated by overlapping WMH segmentations of each subject and calculating the probability of having WMH in each voxel in this sample. Total and regional brain volumes were estimated using previously established automated labeling pathway (ALP)^{42,43}.

Functional pCASL images were motion corrected (tagged and untagged corrected separately and then together) to the first volume and then to the mean image (rigid transformation). The skull-stripped MPRAGE was coregistered (affine) to the mean ASL image and this transformation was used to subsequently also coregister the ICV mask, and white matter probability map (nearest-neighbor interpolation for ICV mask). ASL data was smoothed with a Gaussian kernel with full width at half maximum (FWHM) of 8 mm. Similar processing was also performed on the M0 image. Participants exhibited little in-scanner motion (below 2mm translation). White matter masks were generated by thresholding the white matter probability map at 0.6. CBF was then calculated using ASL toolbox⁴⁴. The following parameters were input: simple subtraction type (tagged-untagged), labeling time 1.16s, delay time 1.1s, slice time 43.5ms, labeling efficiency 0.85, and TE of 13ms. ICV mask was used to determine where to calculate CBF while the white matter mask was used to determine the equilibrium magnetization of white matter.

Mean CBF images were coregistered to the skull stripped MPRAGE via the mean ASL image (affine) and then subsequently was normalized to MNI space using the deformation field (4mm isotropic). Considering the inaccuracy of CBF measurements in white matter^{45,46} and extreme values, we limited CBF within gray matter and included values between 0–200. The threshold gray matter CBF maps were divided by the mean CBF in gray matter to control for the individual differences in mean gray matter CBF. We wanted to also investigate whether the mean CBF map was a reliable indicator of CBF, so for each

individual, we computed a voxel-wise map that indicated the percent of volumes that had a value greater than 3 standard deviations from the mean and found that within the significant region – a *maximum* 7.5% of volumes had values 3 standard deviations above the mean, which translates to approximately 3 volumes. On average, most individuals only had a single volume whose value was 3 standard deviations above the mean CBF. This indicated that the mean CBF was stable.

Statistical Analysis:

Group differences in demographic/clinical variables between remitters and non-remitters were tested using Mann-Whitney U-test or Fisher's exact test in SPSS24.0 (Statistical Package for the Social Sciences).

Voxel-wise analyses were conducted using SnPM13 (<http://warwick.ac.uk/snpm>) and utilized permutation testing (5,000 permutations). All voxel-wise analyses used a cluster forming threshold of $p < 0.005$ and then were corrected to control for family-wise error (FWE, $p < 0.05$). While these results passed cluster-wise significance testing, in response to Eklund et al.⁴⁷, we also report that these results did not pass voxel-wise FWE.

Our primary analysis involved testing the association between the change in MADRS (or remission group) and change in CBF (baseline vs. end). We also investigated whether the placebo, acute (single dose), or subacute (after a week) changes in CBF were associated with total change in MADRS and that this was not dependent on serum venlafaxine levels or years lived with depression (the number of years between current age and age of first lifetime episode of depression). Other exploratory analyses were done to (1) investigate associations with mean gray matter CBF (as this may be driving local differences); (2) investigate associations with baseline CBF; and (3) explore potential confounding variables and adjust for them in the primary analysis.

Another exploratory analysis was conducted to understand baseline CBF and its correlates, thus we conducted a series of analyses using only the baseline CBF. We conducted regressions to investigate the association between baseline CBF and baseline/change in MADRS as well as years lived with depression. We conducted an independent t-test to investigate baseline CBF differences between remission groups.

As the voxel-wise CBF is measure relative to the mean gray matter CBF, we conducted an exploratory analysis to investigate whether there were any associations (as these may be driving local differences) with mean gray matter CBF (baseline or change) and MADRS, years lived with depression, remission group, and blood venlafaxine levels. We also tested for any associations with MADRS (baseline or change) using Mann-Whitney U-tests, Pearson's, or Spearman's rank correlation. We performed false discovery rate (FDR) correction ($\alpha < 0.05$) to control for multiple comparisons⁴⁸.

To explore potential confounds, we investigated whether there were any regional associations between baseline or change in CBF and the following: age, sex, race, education, MMSE, CIRSG, baseline WMH, and WMH changes (slope of change in WMH). After these analyses, we found covariates that were significantly associated with either baseline CBF or

CBF change. We conducted a final model to test the association between CBF and MADRS that adjusted for all the significant covariates simultaneously.

Results

Demographic:

All participants showed improvement in MADRS following a 12-week treatment and 24 met remission criteria. As expected, there were significant differences between remitters and non-remitters in end of trial MADRS, end of trial venlafaxine serum levels, and percent change in MADRS (Table 1).

Significant Voxel-wise CBF Associations:

We found a significant negative association between total changes in CBF (baseline vs. end) and percent change in MADRS in multiple structures (angular/supramarginal gyrus, middle and posterior cingulate, and precuneus; not shown). In this region, we found that sex and MMSE were also associated. After adjusting for sex and MMSE, we found that increased CBF in middle/posterior cingulate, precuneus, angular/supramarginal gyrii, middle/superior frontal gyrii, supplemental motor area, and inferior/superior parietal lobes was significantly associated with improvement in MADRS (depression severity) even after adjusting for sex and MMSE (Figure 2B and Table 2).

Mean CBF from this cluster is plotted it by remission group across the study (Figure 2C). Further, we plotted the negative association between the CBF total change and percent change in MADRS for both groups (Figure 2D). Finally, we overlaid the significant cluster alongside the WMH probability map to demonstrate the spatial relationship (Figure 2E).

Summary of Null Findings:

Importantly, we did not find any association between total changes in CBF (baseline vs. end) and years lived with depression, remission group, venlafaxine serum levels, or baseline MADRS. We found no associations between percent changes in MADRS (baseline vs. end) and changes in CBF following placebo, first dose of venlafaxine, or a week after treatment (i.e. changes occurred in a later period). In our exploratory analysis, we found no significant associations between baseline CBF and baseline MADRS, percent change in MADRS, years lived with depression, or group.

Associations with Mean Gray Matter CBF:

As voxel-wise CBF is relative to mean gray matter CBF, it is possible that these local associations are driven more by the global factor. Thus, we investigated the associations between mean gray matter CBF and depression severity, years lived with depression, and venlafaxine metabolite levels – as well as the associations between the changes in these measures (supplement Table 1). After correcting for multiple comparisons (FDR), we found no significant associations. However, we did observe that total change in depression severity was associated ($p=0.03$, uncorrected) with total change in mean gray matter CBF. (Figure 2A)

Discussion

In this 12-week open-label trial of venlafaxine for LLD we observed an association between increased CBF and depressive symptom improvement. The changes in CBF were detected in midline structures: the middle cingulate, precuneus, and posterior cingulate cortex. Although we did not detect early (less than 1 week) regional CBF changes, we demonstrated a robust association between CBF changes and MADRS changes over the entire 12-week venlafaxine treatment trial.

Previous studies demonstrate that cerebral hypoperfusion is common in aging^{49,50}, that vascular diseases or vascular risk factors are associated with LLD^{51–53}, and that LLD individuals show lower global or regional CBF compared with healthy controls^{31–34}. In general, several studies point to a hypoperfusion in the frontal and limbic cortex as well as the parietal cortex, including the: anterior cingulate^{31,54,55}, posterior cingulate^{55,56}, frontal cortex (SFG, MFG, inferior frontal gyrus or IFG, dIPFC, OFG)^{31,34,54,55,57–59}, motor/sensory cortex^{31,55}, hippocampus³¹, temporal cortex^{31,34,55–59}, SMG³¹, parietal cortex (IPG, superior parietal gyrus or SPG)^{55,57–59}, caudate^{31,55,60}, and thalamus⁶⁰. From this perspective, it may mean that these are normalizing changes (as these may be hypoperfused), however we do not test this explicitly (as we lack a never-depressed group). We also identified three other studies exploring ASL-defined CBF in LLD investigating treatment response^{61–63}. All have used baseline ASL to explain variability in treatment response and showed mixed results, where higher or lower baseline CBF in some regions associated with worse treatment outcome. Since CBF is not a static measure within an individual, but rather can vary with depressive state, the change in CBF over the course of treatment may be more predictive of remission than baseline. Thus, in the current study we focused on the change in CBF over the course of treatment. Our study investigated the CBF trajectory following LLD antidepressant treatment. Our results supported the vascular depression model, by showing that changes in CBF were associated with symptom improvement^{64,65}. Past studies have shown increased perfusion in the precuneus/parietal cortex after successful remission^{32,66}, which aligns well with our own results however there are multiple other regions (that we did not find) that have shown an increased perfusion following successful remission including: left dorsolateral prefrontal cortex and precentral regions³², basal ganglia⁶⁷, anterior cingulate cortex⁶⁷, dorsal anterior cingulate^{68–70}, left superior frontal⁶⁶, and temporal cortex⁶⁶.

Previous studies have shown associations between WMH burden and the treatment response in LLD^{71,72}, and others have shown an association of WMH burden and ASL measures (higher WMH is associated with lower CBF)^{73–75}. However, our current study did not find an association between baseline or change of CBF and WMH burden. This may also be due to a lower effect size of these associations and the limited temporal scope of the observations (previous studies investigated changes across years). The subtle effect of WMH could still lead to hypoperfusion in and around the middle and posterior cingulate, regions which are reported to be the most vulnerable to changes in blood flow due to specific anatomical vascularization⁷⁶. This was partially supported by the co-localization of the significant CBF alteration region and the WMH probability map (Figure 2E).

Recently, our group has reported that there exist early changes in resting-state connectivity following a single dose of medication¹⁷. In the current study the difference in CBF is not apparent before the first week (though it's possible that these changes occur before 12 weeks). This may be due to the longer latency in changes in CBF compared with potentially brisker changes in neuronal activity and connectivity, changes known to be sensitive to acute pharmacotherapy⁷⁷⁻⁷⁹. The ASL signal is less sensitive to acute change compared with BOLD signal, which might be due to less time-varying changes and lower overall temporal resolution (e.g., mean perfusion across five minutes of scanning was calculated in ASL) compared with BOLD. However, this may also mean that the changes in connectivity are related to a required mechanism to remission, while the CBF (as they are lagged) may reflect a change that occurs as a result. In our study where we found changes in connectivity, we used a region of interest (ROI) connectivity analysis, which included a posterior cingulate ROI. While these results may be associated, it is less likely as the cingulate ROI (ventral aspect of the posterior cingulate) from our previous work and the identified regions in this analysis (more dorsal aspect of the posterior cingulate) do not overlap. It is possible that the change in CBF may be more directly linked to depressive state rather than the action of the drug itself. Further studies with a larger sample and more frequent assessments may allow detection of early CBF changes that could potentially serve as treatment predictors.

One possible interpretation, is that the increase in CBF in these areas might reflect a correction for hypoperfusion in deep watershed areas. These areas, near the centrum semi-ovale, are affected to a greater degree by small vessel disease (evidenced by WMH burden), which are associated with decreased CBF. This study supports a relationship between cerebral blood flow and depression but cannot distinguish the direction of the relationship. A longitudinal study with longer-term follow-up could help distinguish the principal direction of the relationship of CBF and depressive symptoms. The posterior cingulate is a core node in the default node network, a network of primarily mid-line structures which shows high connectivity during task-free states. Functional MRI studies using the BOLD contrast have shown impaired functioning of the DMN. The CBF changes could help explain the cause of the DMN functional alterations in vascular depression. Decreased perfusion of these regions may lead to functional alterations in the circuit.

The present study has several limitations. The first is a relatively small sample size – thus requiring further verification and replication. Related to a small sample size, we have used a cluster-wise family wise error (FWE) correction to control for multiple comparisons and a non-parametric permutation approach that is in-line with the current literature regarding multiple comparisons correction⁴⁷. We have used a delay time of 1.1 seconds, which may be too short in elderly participants according to recent consensus work (that suggested 2 seconds instead)⁸⁰ – this may mean that the signal is primarily generated inside the blood vessels. As our data was collected prior to this work, we are unable to adjust for this and thus our result should be interpreted within this context. Due to this, we cannot rule out that there does not exist an early change, as well as an association between CBF and WMH. Second, associations were computed using regression and thus do not imply causal links. Moreover, past studies have showed that hypertension was associated with a decline in CBF, while patients who were successfully treated for their hypertension did not show such a decline⁸¹. The mechanism may be that the chronic stress of hypertension causes thickening

and hardening of the walls of arterioles with narrowing of lumen, and leads to cerebral hypoperfusion⁸². In the context of the vascular depression hypothesis, the blood pressure should be well controlled in an effort to protect the cerebral arteries and prevent and treat LLD. But the hypertension and CBF relationship cannot be verified in the presented study due to an absence of blood pressure data.

In conclusion, this is the first study investigating the trajectory of CBF alteration following LLD pharmacotherapy. The measurement of CBF using ASL is a promising tool for understanding the biological mechanisms of LLD. The association between increased CBF in precuneus, posterior cingulate, and middle cingulate and symptom improvement further supports the vascular depression hypothesis. Besides external validation in an independent sample with measurements of blood pressure and other relevant cardiovascular features, there are several critical aspects that have yet to be addressed and should be addressed in future studies. While we showed changes in CBF, it is unclear how these changes relate to long-term changes in WMH, relapse, and even future CBF – it is possible that treatment partially improves the continuing cycle of high depressive symptoms-low CBF-high WMH. Also, while we showed that there does exist an association between depressive symptoms and CBF, we did not address the directional aspect of this change and whether the change in symptoms improves CBF or the change in CBF improves symptoms. This would require a neuroimaging study with multiple time points during the 3–8 week period, which we did not have. Also, how do changes in CBF affect changes in connectivity and vice-versa and whether these changes necessary for improvement of depressive symptoms or just a consequence. Finally, future studies should also directly investigate the association between age of onset and CBF – this is an under-represented area of research with studies mainly reporting differences in WMH.

Supplementary Material

Refer to Web version on PubMed Central for supplementary material.

Acknowledgement:

This study was funded by NIMH R01 MH076079, 5R01 AG033575, K23 MH086686, P30 MH90333, 5R01 MH083660 and T32 MH019986. The sponsors had no role in the design, implementation, analysis, or interpretation of these data. The authors declare no conflicts of interest.

References

1. Ferrari AJ, Charlson FJ, Norman RE, et al. Burden of depressive disorders by country, sex, age, and year: findings from the global burden of disease study 2010. *PLoS Med.* 2013;10(11):e1001547. [PubMed: 24223526]
2. Murray CJ, Lopez AD. Alternative projections of mortality and disability by cause 1990–2020: Global Burden of Disease Study. *Lancet.* 1997;349(9064):1498–1504. [PubMed: 9167458]
3. Gottfries CG. Late life depression. *Eur Arch Psychiatry Clin Neurosci.* 2001;251 Suppl 2:II57–61. [PubMed: 11824838]
4. Djernes JK. Prevalence and predictors of depression in populations of elderly: a review. *Acta Psychiatr Scand.* 2006;113(5):372–387. [PubMed: 16603029]
5. Beekman AT, Copeland JR, Prince MJ. Review of community prevalence of depression in later life. *Br J Psychiatry.* 1999;174:307–311. [PubMed: 10533549]

6. Kok RM, Nolen WA, Heeren TJ. Efficacy of treatment in older depressed patients: a systematic review and meta-analysis of double-blind randomized controlled trials with antidepressants. *J Affect Disord.* 2012;141(2–3):103–115. [PubMed: 22480823]
7. Cooper C, Katona C, Lyketsos K, et al. A systematic review of treatments for refractory depression in older people. *Am J Psychiatry.* 2011;168(7):681–688. [PubMed: 21454919]
8. Sneed JR, Rutherford BR, Rindskopf D, Lane DT, Sackeim HA, Roose SP. Design makes a difference: a meta-analysis of antidepressant response rates in placebo-controlled versus comparator trials in late-life depression. *Am J Geriatr Psychiatry.* 2008;16(1):65–73. [PubMed: 17998306]
9. Kok RM, Reynolds CF, 3rd. Management of Depression in Older Adults: A Review. *JAMA.* 2017;317(20):2114–2122. [PubMed: 28535241]
10. Andreescu C, Reynolds CF, 3rd. Late-life depression: evidence-based treatment and promising new directions for research and clinical practice. *Psychiatr Clin North Am.* 2011;34(2):335–355, vii–iii. [PubMed: 21536162]
11. Pizzagalli DA. Frontocingulate dysfunction in depression: toward biomarkers of treatment response. *Neuropsychopharmacology.* 2011;36(1):183–206. [PubMed: 20861828]
12. Ribeiz SR, Duran F, Oliveira MC, et al. Structural brain changes as biomarkers and outcome predictors in patients with late-life depression: a cross-sectional and prospective study. *PLoS One.* 2013;8(11):e80049. [PubMed: 24244606]
13. Sheline YI, Disabato BM, Hranilovich J, et al. Treatment course with antidepressant therapy in late-life depression. *Am J Psychiatry.* 2012;169(11):1185–1193. [PubMed: 23534057]
14. Taylor WD, Kuchibhatla M, Payne ME, et al. Frontal white matter anisotropy and antidepressant remission in late-life depression. *PLoS One.* 2008;3(9):e3267. [PubMed: 18813343]
15. Aizenstein HJ, Khalaf A, Walker SE, Andreescu C. Magnetic resonance imaging predictors of treatment response in late-life depression. *J Geriatr Psychiatry Neurol.* 2014;27(1):24–32. [PubMed: 24381231]
16. Fu CH, Steiner H, Costafreda SG. Predictive neural biomarkers of clinical response in depression: a meta-analysis of functional and structural neuroimaging studies of pharmacological and psychological therapies. *Neurobiol Dis.* 2013;52:75–83. [PubMed: 22659303]
17. Karim HT, Andreescu C, Tudorascu D, et al. Intrinsic functional connectivity in late-life depression: trajectories over the course of pharmacotherapy in remitters and non-remitters. *Mol Psychiatry.* 2017;22(3):450–457. [PubMed: 27090303]
18. Alexopoulos GS, Meyers BS, Young RC, Campbell S, Silbersweig D, Charlson M. ‘Vascular depression’ hypothesis. *Arch Gen Psychiatry.* 1997;54(10):915–922. [PubMed: 9337771]
19. Pantoni L. Cerebral small vessel disease: from pathogenesis and clinical characteristics to therapeutic challenges. *Lancet Neurol.* 2010;9(7):689–701. [PubMed: 20610345]
20. Papma JM, de Groot M, de Koning I, et al. Cerebral small vessel disease affects white matter microstructure in mild cognitive impairment. *Hum Brain Mapp.* 2014;35(6):2836–2851. [PubMed: 24115179]
21. Kitagawa K, Oku N, Kimura Y, et al. Relationship between cerebral blood flow and later cognitive decline in hypertensive patients with cerebral small vessel disease. *Hypertens Res.* 2009;32(9):816–820. [PubMed: 19575014]
22. Seminowicz DA, Mayberg HS, McIntosh AR, et al. Limbic-frontal circuitry in major depression: a path modeling metanalysis. *Neuroimage.* 2004;22(1):409–418. [PubMed: 15110034]
23. Liang X, Zou Q, He Y, Yang Y. Coupling of functional connectivity and regional cerebral blood flow reveals a physiological basis for network hubs of the human brain. *Proc Natl Acad Sci U S A.* 2013;110(5):1929–1934. [PubMed: 23319644]
24. Chen Y, Wan HI, O’Reardon JP, et al. Quantification of cerebral blood flow as biomarker of drug effect: arterial spin labeling phMRI after a single dose of oral citalopram. *Clin Pharmacol Ther.* 2011;89(2):251–258. [PubMed: 21191380]
25. Borogovac A, Asllani I. Arterial Spin Labeling (ASL) fMRI: advantages, theoretical constrains, and experimental challenges in neurosciences. *Int J Biomed Imaging.* 2012;2012:818456. [PubMed: 22966219]

26. Vasic N, Wolf ND, Gron G, et al. Baseline brain perfusion and brain structure in patients with major depression: a multimodal magnetic resonance imaging study. *J Psychiatry Neurosci*. 2015;40(6):412–421. [PubMed: 26125119]
27. Ota M, Noda T, Sato N, et al. Characteristic distributions of regional cerebral blood flow changes in major depressive disorder patients: a pseudo-continuous arterial spin labeling (pCASL) study. *J Affect Disord*. 2014;165:59–63. [PubMed: 24882178]
28. Chen G, Bian H, Jiang D, et al. Pseudo-continuous arterial spin labeling imaging of cerebral blood perfusion asymmetry in drug-naïve patients with first-episode major depression. *Biomed Rep*. 2016;5(6):675–680. [PubMed: 28101340]
29. Skaf CR, Yamada A, Garrido GE, et al. Psychotic symptoms in major depressive disorder are associated with reduced regional cerebral blood flow in the subgenual anterior cingulate cortex: a voxel-based single photon emission computed tomography (SPECT) study. *J Affect Disord*. 2002;68(2–3):295–305. [PubMed: 12063157]
30. Perico CA, Skaf CR, Yamada A, et al. Relationship between regional cerebral blood flow and separate symptom clusters of major depression: a single photon emission computed tomography study using statistical parametric mapping. *Neurosci Lett*. 2005;384(3):265–270. [PubMed: 15921853]
31. Awata S, Ito H, Konno M, et al. Regional cerebral blood flow abnormalities in late-life depression: relation to refractoriness and chronification. *Psychiatry Clin Neurosci*. 1998;52(1):97–105. [PubMed: 9682941]
32. Ishizaki J, Yamamoto H, Takahashi T, Takeda M, Yano M, Mimura M. Changes in regional cerebral blood flow following antidepressant treatment in late-life depression. *Int J Geriatr Psychiatry*. 2008;23(8):805–811. [PubMed: 18214999]
33. Navarro V, Gasto C, Lomena F, Mateos JJ, Marcos T. Frontal cerebral perfusion dysfunction in elderly late-onset major depression assessed by 99mTc-HMPAO SPECT. *Neuroimage*. 2001;14(1 Pt 1):202–205. [PubMed: 11525329]
34. Lesser IM, Mena I, Boone KB, Miller BL, Mehringer CM, Wohl M. Reduction of cerebral blood flow in older depressed patients. *Arch Gen Psychiatry*. 1994;51(9):677–686. [PubMed: 8080344]
35. Alexopoulos GS. Depression in the elderly. *Lancet*. 2005;365(9475):1961–1970. [PubMed: 15936426]
36. Taylor WD, Aizenstein HJ, Alexopoulos GS. The vascular depression hypothesis: mechanisms linking vascular disease with depression. *Mol Psychiatry*. 2013;18(9):963–974. [PubMed: 23439482]
37. Xu G, Rowley HA, Wu G, et al. Reliability and precision of pseudo-continuous arterial spin labeling perfusion MRI on 3.0 T and comparison with 15O-water PET in elderly subjects at risk for Alzheimer's disease. *NMR Biomed*. 2010;23(3):286–293. [PubMed: 19953503]
38. Lenze EJ, Mulsant BH, Blumberger DM, et al. Efficacy, safety, and tolerability of augmentation pharmacotherapy with aripiprazole for treatment-resistant depression in late life: a randomised, double-blind, placebo-controlled trial. *Lancet*. 2015;386(10011):2404–2412. [PubMed: 26423182]
39. Karp JF, Rollman BL, Reynolds CF, 3rd, et al. Addressing both depression and pain in late life: the methodology of the ADAPT study. *Pain Med*. 2012;13(3):405–418. [PubMed: 22313547]
40. Miller MD, Paradis CF, Houck PR, et al. Rating chronic medical illness burden in geropsychiatric practice and research: application of the Cumulative Illness Rating Scale. *Psychiatry Res*. 1992;41(3):237–248. [PubMed: 1594710]
41. Folstein MF, Folstein SE, McHugh PR. "Mini-mental state". A practical method for grading the cognitive state of patients for the clinician. *J Psychiatr Res*. 1975;12(3):189–198. [PubMed: 1202204]
42. Wu M, Rosano C, Butters M, et al. A fully automated method for quantifying and localizing white matter hyperintensities on MR images. *Psychiatry Res*. 2006;148(2–3):133–142. [PubMed: 17097277]
43. Wu M, Carmichael O, Lopez-Garcia P, Carter CS, Aizenstein HJ. Quantitative comparison of AIR, SPM, and the fully deformable model for atlas-based segmentation of functional and structural MR images. *Hum Brain Mapp*. 2006;27(9):747–754. [PubMed: 16463385]

44. Wang Z, Aguirre GK, Rao H, et al. Empirical optimization of ASL data analysis using an ASL data processing toolbox: ASLtbx. *Magn Reson Imaging*. 2008;26(2):261–269. [PubMed: 17826940]
45. van Osch MJ, Teeuwisse WM, van Walderveen MA, Hendrikse J, Kies DA, van Buchem MA. Can arterial spin labeling detect white matter perfusion signal? *Magn Reson Med*. 2009;62(1):165–173. [PubMed: 19365865]
46. van Gelderen P, de Zwart JA, Duyn JH. Pitfalls of MRI measurement of white matter perfusion based on arterial spin labeling. *Magn Reson Med*. 2008;59(4):788–795. [PubMed: 18383289]
47. Eklund A, Nichols TE, Knutsson H. Cluster failure: Why fMRI inferences for spatial extent have inflated false-positive rates. *Proc Natl Acad Sci U S A*. 2016;113(28):7900–7905. [PubMed: 27357684]
48. Hochberg Y, Benjamini Y. More powerful procedures for multiple significance testing. *Stat Med*. 1990;9(7):811–818. [PubMed: 2218183]
49. Yang D, Cabral D, Gaspard EN, Lipton RB, Rundek T, Derby CA. Cerebral Hemodynamics in the Elderly: A Transcranial Doppler Study in the Einstein Aging Study Cohort. *J Ultrasound Med*. 2016;35(9):1907–1914. [PubMed: 27417737]
50. Zhang N, Gordon ML, Goldberg TE. Cerebral blood flow measured by arterial spin labeling MRI at resting state in normal aging and Alzheimer's disease. *Neurosci Biobehav Rev*. 2017;72:168–175. [PubMed: 27908711]
51. van Agtmaal MJM, Houben A, Pouwer F, Stehouwer CDA, Schram MT. Association of Microvascular Dysfunction With Late-Life Depression: A Systematic Review and Meta-analysis. *JAMA Psychiatry*. 2017.
52. Gothe F, Enache D, Wahlund LO, et al. Cerebrovascular diseases and depression: epidemiology, mechanisms and treatment. *Panminerva Med*. 2012;54(3):161–170. [PubMed: 22801433]
53. Valkanova V, Ebmeier KP. Vascular risk factors and depression in later life: a systematic review and meta-analysis. *Biol Psychiatry*. 2013;73(5):406–413. [PubMed: 23237315]
54. Bench CJ, Friston KJ, Brown RG, Frackowiak RS, Dolan RJ. Regional cerebral blood flow in depression measured by positron emission tomography: the relationship with clinical dimensions. *Psychol Med*. 1993;23(3):579–590. [PubMed: 7901863]
55. Kumar A, Newberg A, Alavi A, Berlin J, Smith R, Reivich M. Regional cerebral glucose metabolism in late-life depression and Alzheimer disease: a preliminary positron emission tomography study. *Proc Natl Acad Sci U S A*. 1993;90(15):7019–7023. [PubMed: 8346211]
56. Ebmeier KP, Glabus MF, Prentice N, Ryman A, Goodwin GM. A voxel-based analysis of cerebral perfusion in dementia and depression of old age. *Neuroimage*. 1998;7(3):199–208. [PubMed: 9597661]
57. Nobler MS, Roose SP, Prohovnik I, et al. Regional cerebral blood flow in mood disorders, V.: Effects of antidepressant medication in late-life depression. *Am J Geriatr Psychiatry*. 2000;8(4):289–296. [PubMed: 11069268]
58. Sackeim HA, Prohovnik I, Moeller JR, et al. Regional cerebral blood flow in mood disorders. I. Comparison of major depressives and normal controls at rest. *Arch Gen Psychiatry*. 1990;47(1):60–70. [PubMed: 2294857]
59. Upadhyaya AK, Abou-Saleh MT, Wilson K, Grime SJ, Critchley M. A study of depression in old age using single-photon emission computerised tomography. *Br J Psychiatry Suppl*. 1990(9):76–81. [PubMed: 2291822]
60. Curran SM, Murray CM, Van Beck M, et al. A single photon emission computerised tomography study of regional brain function in elderly patients with major depression and with Alzheimer-type dementia. *Br J Psychiatry*. 1993;163:155–165. [PubMed: 8075905]
61. Colloby SJ, Firbank MJ, He J, et al. Regional cerebral blood flow in late-life depression: arterial spin labelling magnetic resonance study. *Br J Psychiatry*. 2012;200(2):150–155. [PubMed: 22194184]
62. Abi Zeid Daou M, Boyd BD, Donahue MJ, Albert K, Taylor WD. Frontocingulate cerebral blood flow and cerebrovascular reactivity associated with antidepressant response in late-life depression. *J Affect Disord*. 2017;215:103–110. [PubMed: 28324779]
63. Liao W, Wang Z, Zhang X, et al. Cerebral blood flow changes in remitted early- and late-onset depression patients. *Oncotarget*. 2017;8(44):76214–76222. [PubMed: 29100305]

64. Awata S, Konno M, Kawashima R, et al. Changes in regional cerebral blood flow abnormalities in late-life depression following response to electroconvulsive therapy. *Psychiatry Clin Neurosci*. 2002;56(1):31–40. [PubMed: 11929569]
65. Bonne O, Krausz Y, Shapira B, et al. Increased cerebral blood flow in depressed patients responding to electroconvulsive therapy. *J Nucl Med*. 1996;37(7):1075–1080. [PubMed: 8965172]
66. Ogura A, Morinobu S, Kawakatsu S, Totsuka S, Komatani A. Changes in regional brain activity in major depression after successful treatment with antidepressant drugs. *Acta Psychiatr Scand*. 1998;98(1):54–59. [PubMed: 9696515]
67. Goodwin GM, Austin MP, Dougall N, et al. State changes in brain activity shown by the uptake of ^{99m}Tc-exametazime with single photon emission tomography in major depression before and after treatment. *J Affect Disord*. 1993;29(4):243–253. [PubMed: 8126311]
68. Bench CJ, Frackowiak RS, Dolan RJ. Changes in regional cerebral blood flow on recovery from depression. *Psychol Med*. 1995;25(2):247–261. [PubMed: 7675913]
69. Buchsbaum MS, Wu J, Siegel BV, et al. Effect of sertraline on regional metabolic rate in patients with affective disorder. *Biol Psychiatry*. 1997;41(1):15–22. [PubMed: 8988791]
70. Mayberg HS, Liotti M, Brannan SK, et al. Reciprocal limbic-cortical function and negative mood: converging PET findings in depression and normal sadness. *Am J Psychiatry*. 1999;156(5):675–682. [PubMed: 10327898]
71. Herrmann LL, Le Masurier M, Ebmeier KP. White matter hyperintensities in late life depression: a systematic review. *J Neurol Neurosurg Psychiatry*. 2008;79(6):619–624. [PubMed: 17717021]
72. Khalaf A, Edelman K, Tudorascu D, Andreescu C, Reynolds CF, Aizenstein H. White Matter Hyperintensity Accumulation During Treatment of Late-Life Depression. *Neuropsychopharmacology*. 2015;40(13):3027–3035. [PubMed: 26058663]
73. Brickman AM, Zahra A, Muraskin J, et al. Reduction in cerebral blood flow in areas appearing as white matter hyperintensities on magnetic resonance imaging. *Psychiatry Res*. 2009;172(2):117–120. [PubMed: 19324534]
74. ten Dam VH, van den Heuvel DM, de Craen AJ, et al. Decline in total cerebral blood flow is linked with increase in periventricular but not deep white matter hyperintensities. *Radiology*. 2007;243(1):198–203. [PubMed: 17329688]
75. Crane DE, Black SE, Ganda A, et al. Gray matter blood flow and volume are reduced in association with white matter hyperintensity lesion burden: a cross-sectional MRI study. *Front Aging Neurosci*. 2015;7:131. [PubMed: 26217223]
76. Tatu L, Moulin T, Vuillier F, Bogousslavsky J. Arterial territories of the human brain. *Front Neurol Neurosci*. 2012;30:99–110. [PubMed: 22377874]
77. Outhred T, Das P, Felmingham KL, et al. Facilitation of emotion regulation with a single dose of escitalopram: A randomized fMRI study. *Psychiatry Res*. 2015;233(3):451–457. [PubMed: 26210693]
78. Cremers H, Lee R, Keedy S, Phan KL, Coccaro E. Effects of Escitalopram Administration on Face Processing in Intermittent Explosive Disorder: An fMRI Study. *Neuropsychopharmacology*. 2016;41(2):590–597. [PubMed: 26105140]
79. Klaassens BL, van Gorsel HC, Khalili-Mahani N, et al. Single-dose serotonergic stimulation shows widespread effects on functional brain connectivity. *Neuroimage*. 2015;122:440–450. [PubMed: 26277774]
80. Alsop DC, Detre JA, Golay X, et al. Recommended implementation of arterial spin-labeled perfusion MRI for clinical applications: A consensus of the ISMRM perfusion study group and the European consortium for ASL in dementia. *Magn Reson Med*. 2015;73(1):102–116. [PubMed: 24715426]
81. Muller M, van der Graaf Y, Visseren FL, Mali WP, Geerlings MI, Group SS. Hypertension and longitudinal changes in cerebral blood flow: the SMART-MR study. *Ann Neurol*. 2012;71(6):825–833. [PubMed: 22447734]
82. Novak V, Chowdhary A, Farrar B, et al. Altered cerebral vasoregulation in hypertension and stroke. *Neurology*. 2003;60(10):1657–1663. [PubMed: 12771258]

Clinical Points:

- Increased white matter hyperintensities (WMH) are associated with decreased cerebral blood flow (CBF) in late-life depression (LLD). We found that CBF increases following treatment in regions that are typically more affected by WMH (as some past studies have found) but failed to identify early (within a week) changes.
- The vascular depression hypothesis posits that cerebrovascular disease may predispose, precipitate, or perpetuate depressive symptoms in late-life. Though we do not test this directly, we believe that remission may partially break this cycle due to increased CBF in these afflicted areas. The direct mechanism by which this occurs is still unclear.

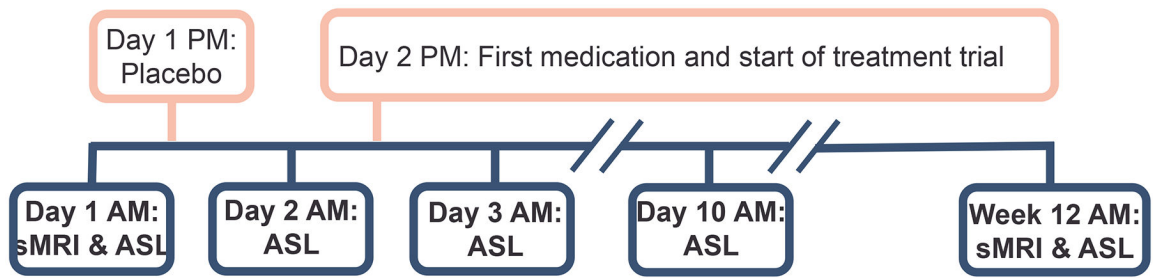


Figure 1.

The study design protocol. Five magnetic resonance imaging (MRI) scans (in blue) were performed throughout the course of treatment (in pink). All scanning was done in the morning. (sMRI, structural MRI; ASL, arterial spin labeling)

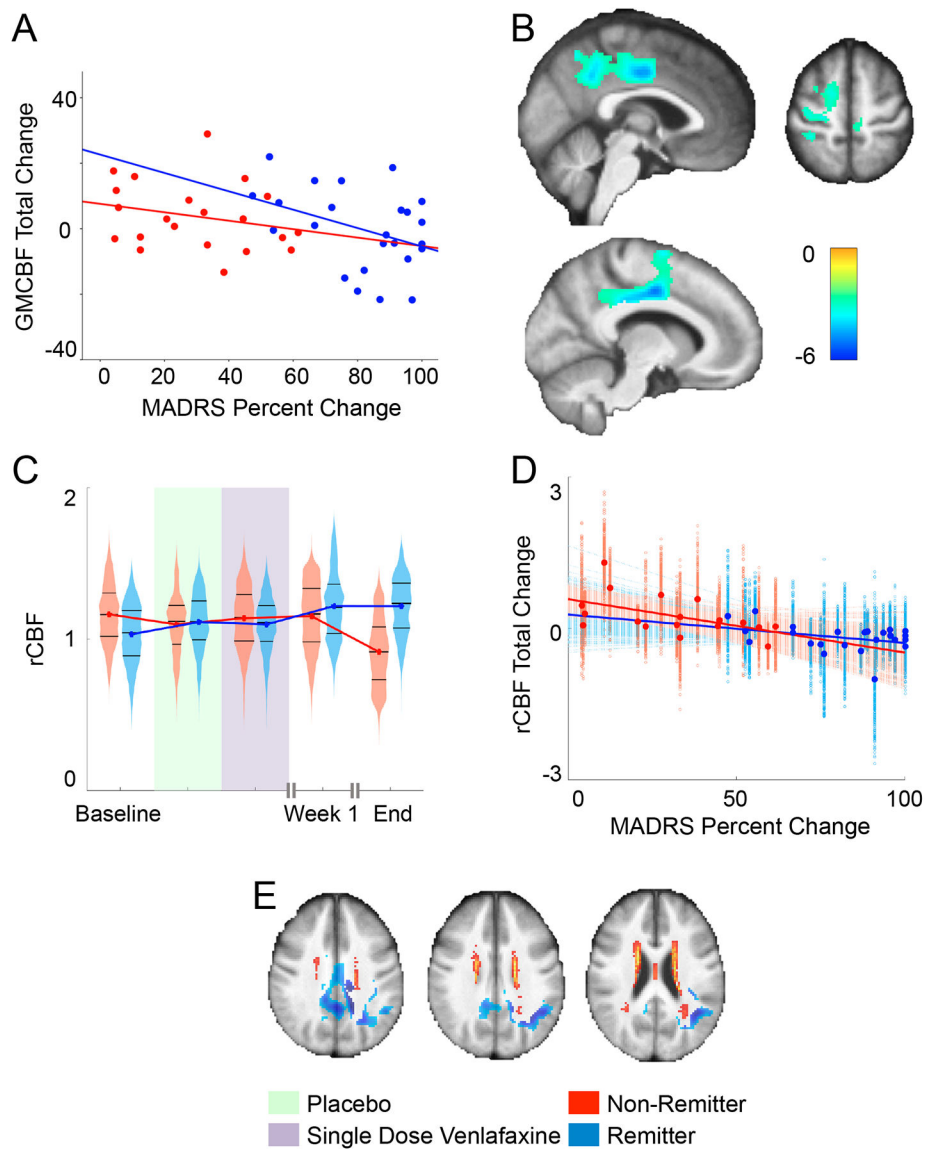


Figure 2.

(A) We calculated the mean CBF within the significant cluster that survived the previous analysis and plotted the trajectories of mean CBF at each time point in remitters and non-remitters. The association between the total change in mean gray matter cerebral blood flow (GMCBF) and the total percent change in MADRS ($p=0.03$, uncorrected). (B) Cluster that showed significant association between overall CBF difference and overall MADRS percent change, independent of gender and MMSE overlaid on mean structural image (5000 permutations, cluster forming threshold $p<0.005$, FWE corrected $p<0.05$). (C) Trajectories of ROI mean regional CBF (rCBF) change in remitters and non-remitters. To better indicate the variability across this cluster, we also used violin plots that show a mirrored histogram alongside the median and 25th and 75th percentiles (black lines). (D) The CBF change from baseline to end of trial was negatively associated with MADRS percent change from baseline to end of trial. To better indicate the variability across this cluster, each voxel-wise

point is presented alongside each voxel-wise best-fit line, while the larger highlighted points are the mean CBF and bold best-fit lines are fit to that as well. **(E)** The significant cluster and WMH probability map overlaid on the mean structural image to demonstrate their spatial relationship.

Table 1.

Group differences in demographic and clinical variables between remitters and non-remitters.

	Non-Remitters (N = 22)	Remitters (N = 24)	Group Comparison
Age (median, IQR)	64.5 (8.0)	66.0 (11.5)	p = 0.574
Race (CC/AA)	18/4	20/4	p = 1.000
Gender (female)	11	18	p = 0.126
Education (median, IQR)	16.0 (2.0)	13.0 (6.0)	p = 0.269
MMSE (median, IQR)	29.0 (1.8) ^c	29.0 (2.0)	p = 0.857
CIRSG Total (median, IQR)	8.0 (4.8) ^e	9.0 (4.3) ^c	p = 0.918
CIRSG Vascular Item (median, IQR)	2.0 (2.0)	2.0 (2.0)	p = 0.818
Depression Onset Age (median, IQR)	30 (32) ^a	43 (39.3) ^c	p = 0.563
Years lived with depression (median, IQR)	31.0 (32.3) ^a	25.0 (42.3) ^c	p = 0.772
Depression Type (single/recurrent)	11/9	7/16 ^a	p = 0.130
MADRS Baseline (median, IQR)	27.0 (7)	23.5 (11)	p = 0.069
MADRS 1 Week (median, IQR)	24.5 (7)	19.5 (10.5)	p = 0.034 *
MADRS End (median, IQR)	20.0 (8.5) ^a	3 (6)	p < 0.001 *
MADRS Change Ratio (median, IQR)(%)	32.3 (33.0) ^a	87.5 (26.2)	p < 0.001 *
Venlafaxine Level 1 st Dose (median, IQR)(ng/ml)	26.0 (14.4) ^e	21.0 (13.5) ^d	p = 0.185
Venlafaxine Level 1 Week (median, IQR)(ng/ml)	102.5 (103) ^b	75.0 (23.9) ^a	p = 0.381
Venlafaxine Level End (median, IQR)(ng/ml)	270.0 (355.8) ^b	107.5 (138) ^b	p = 0.003 *
CBF Baseline (median, IQR)	43.3 (19.1)	46.5 (13.7)	p = 0.429
CBF Change (median, IQR)	2.8 (12.9)	0.3 (15.8)	p = 0.403

* Significant (p < 0.05) differences;

^aOne,^bTwo,^cThree,^dFour, or^eFive participant's data was missing;

Abbreviations: IQR, interquartile range; CC, Caucasian; AA, African American; MMSE, mini-mental state examination; CIRSG, cumulative illness rating scale for geriatrics; MADRS, Montgomery-Åsberg Depression Rating Scale; the group comparisons of race, gender, and depression type were conducted with Fisher's exact test, while others with Mann-Whitney U test.

Table 2.

Report of regions (part of a single cluster) that showed significant association between overall CBF difference and overall MADRS percent change, independent of gender and MMSE.

Region of Interest	Brodman Area	Number of Voxels	Tmax (df = 38)	Coordinate of Peak (x,y,z)
Right hemisphere				
Angular/Supramarginal		229	4.25	-40, -50, 26
Middle Cingulate	24, 31	1008	4.92	-10, -8, 42
Posterior Cingulate		74	3.75	0, -46, 34
Middle Frontal		55	3.13	-24, -4, 52
Superior Frontal		160	3.88	-18, 0, 54
Middle Occipital		123	3.73	-26, -56, 34
Inferior Parietal		182	3.90	-36, -32, 40
Superior Parietal		78	3.31	-20, -54, 46
Post-central		201	3.87	-36, -34, 42
Pre-central		178	3.57	-22, -22, 62
Precuneus	7	403	4.33	-2, -48, 38
Supplemental Motor/Medial Frontal	6	289	3.76	-12, -2, 48
Supramarginal		85	3.62	-48, -48, 30
Middle Temporal		79	3.59	-40, -52, 22
Left hemisphere				
Middle Cingulate	31, 24	913	4.42	2, -12, 40
Posterior Cingulate		104	3.46	10, -44, 32
Precuneus/Posterior Cingulate		355	3.85	2, -44, 44